1521-0111/12/8202-156–167$25.00
MOLECULAR PHARMACOLOGY
Copyright © 2012 The American Society for Pharmacology and Experimental Therapeutics
Mol Pharmacol 82:156–167, 2012

Vol. 82, No. 2
78063/3781086

OX_1 Orexin/Hypocretin Receptor Signaling through Arachidonic Acid and Endocannabinoid Release[S]

Pauli M. Turunen, Maria H. Jäntti, and Jyrki P. Kukkonen

Biochemistry and Cell Biology, Department of Veterinary Biosciences, University of Helsinki, Helsinki, Finland

Received February 1, 2012; accepted May 1, 2012

ABSTRACT

We showed previously that OX_1 orexin receptor stimulation produced a strong ^3H overflow response from [^3H]arachidonic acid (AA)-labeled cells. Here we addressed this issue with a novel set of tools and methods, to distinguish the enzyme pathways responsible for this response. CHO-K1 cells heterologously expressing human OX_1 receptors were used as a model system. By using selective pharmacological inhibitors, we showed that, in orexin-A-stimulated cells, the AA-derived radioactivity was released as two distinct components, i.e., free AA and the endocannabinoid 2-arachidonoyl glycerol (2-AG). Two orexin-activated enzymatic cascades are responsible for this response: cytosolic phospholipase A_2 ($cPLA_2$) and diacylglycerol lipase; the former cascade is responsible for part of the AA release, whereas the latter is responsible for all of the 2-AG release and part of the AA release. Essentially only diacylglycerol released by phospholipase C but not by phospholipase D was implicated as a substrate for 2-AG production, although both phospholipases were strongly activated. The 2-AG released acted as a potent paracrine messenger through cannabinoid CB_1 receptors in an artificial cell-cell communication assay that was developed. The $cPLA_2$ cascade, in contrast, was involved in the activation of orexin receptor-operated Ca^{2+} influx. 2-AG was also released upon OX_1 receptor stimulation in recombinant HEK-293 and neuro-2a cells. The results directly show, for the first time, that orexin receptors are able to generate potent endocannabinoid signals in addition to arachidonic acid signals, which may explain the proposed orexin-cannabinoid interactions (e.g., in neurons).

Introduction

The peptide transmitters orexins/hypocretins, which act through G-protein-coupled OX_1 and OX_2 receptors, are involved in the regulation of homeostatic brain functions, especially wakefulness and sleep patterns and appetite (reviewed in Kukkonen et al., 2002; Scammell and Winrow, 2011). Orexin receptor expression and signaling are also found in the periphery of the body, but the physiological significance of this is not known. The molecular mechanisms of orexin receptor signaling are very diverse (reviewed in Kukkonen and Åkerman, 2005). Especially prominent seems to be coupling to the production of messengers through phospholipase action (Johansson et al., 2008; Turunen et al., 2010a; Jäntti et al., 2012).

Endocannabinoids are phospholipid-derived messengers that contain arachidonic acid (AA). The most well established endocannabinoids are 2-arachidonoylglycerol (2-AG) and anandamide (*N*-arachidonoyl-ethanolamine) (reviewed in Kano et al., 2009). Endocannabinoids act through G-protein-coupled CB_1 and CB_2 receptors; the CB_1 receptor is ex-

This study was supported by the Academy of Finland, the Magnus Ehrnrooth Foundation, the University of Helsinki Research Funds, the Biomedicum Helsinki Foundation, and the Research Foundation of the University of Helsinki.

Article, publication date, and citation information can be found at http://molpharm.aspetjournals.org.

http://dx.doi.org/10.1124/mol.112.078063.

[S] The online version of this article (available at http://molpharm.aspetjournals.org) contains supplemental material.

ABBREVIATIONS: AA, arachidonic acid; 2-AG, 2-arachidonoyl glycerol; AM-251, 1-(2,4-dichlorophenyl)-5-(4-iodophenyl)-4-methyl-*N*-1-piperidinyl-1*H*-pyrazole-3-carboxamide; CAY10499, [4-[5-methoxy-2-oxo-1,3,4-oxadiazol-3(2*H*)-yl]-2-methylphenyl]carbamic acid phenylmethyl ester; CAY10593, *N*-[2-[4-(5-chloro-2,3-dihydro-2-oxo-1*H*-benzimidazol-1-yl)-1-piperidinyl]-1-methylethyl]-2-naphthalenecarboxamide; CCPA, *N*-cyclohexanecarbonylpentadecylamine; CHO, Chinese hamster ovary; $cPLA_2$, cytosolic (Ca^{2+}-independent) phospholipase A_2; DAG, diacylglycerol; DAGL, diacylglycerol lipase; FAAH, fatty acid amide hydrolase; FKGK11, 1,1,1,2,2-pentafluoro-7-phenyl-heptan-3-one; HBM, HEPES-buffered medium; HU-210, 3-(1,1′-dimethylheptyl)-6*aR*,7,10,10*aR*-tetrahydro-1-hydroxy-6,6-dimethyl-6*H*-dibenzo[*b*,*d*]pyran-9-methanol; IBMX, 3-isobutyl-1-methylxanthine; $iPLA_2$, intracellular (Ca^{2+}-independent) phospholipase A_2; JZL184, 4-nitrophenyl-4-[dibenzo[*d*][1,3]dioxol-5-yl(hydroxy)methyl]piperidine-1-carboxylate; MAFP, methyl arachidonyl fluorophosphonate; MAGL, monoacylglycerol lipase; PA, phosphatidic acid; PLA_2, phospholipase A_2; PLC, phospholipase C; PLD, phospholipase D; RHC-80267, 1,6-bis(cyclohexyloximinocarbonylamino)hexane; SB-334867, 1-[2-methylbenzoxazol-6-yl]-3-[1,5]naphthyridin-4-yl-urea HCl; S-BSA, stripped bovine serum albumin; THL, tetrahydrolipstatin; TLC, thin-layer chromatography; U-73122, 1-[6-([(17*b*)-3-methoxyestra-1,3,5(10)-trien-17-yl]amino)hexyl]-1*H*-pyrrole-2,5-dione; URB597, [3-(3-carbamoylphenyl)phenyl] *N*-cyclohexylcarbamate.

pressed in central neurons. In addition to the receptors, the endocannabinoid system includes the enzymes that produce and metabolize endocannabinoids. Endocannabinoids are generally thought to be produced on demand and not stored in membrane vesicles like traditional neurotransmitters. Endocannabinoid signaling has been a subject of much interest from both the basic physiological perspective and the medical one. In the central nervous system, endocannabinoids are involved in the regulation of, e.g., appetite, nociception, memory, reward, and mood (reviewed in Kano et al., 2009). On the synaptic level, endocannabinoids engage in retrograde transmission, in which postsynaptically produced endocannabinoids act on the inhibitory, presynaptic CB_1 receptors. This function may also act in homosynaptic feedback, but the assumed major function is heterosynaptic. Cannabinoid receptors couple to G-proteins in the G_i family, and the presynaptic inhibition is likely to occur through $G\beta\gamma$-mediated inhibition of voltage-gated Ca^{2+} channels and inward rectifier K^+ channels (reviewed in Howlett, 2005; Kano et al., 2009).

There is much circumstantial evidence for interactions between orexinergic and cannabinoidergic systems. These systems show significant overlap on the gross neuroanatomical level, especially in particular nuclei of the hypothalamus. However, the possibility of interactions at the cellular level has not been verified for most nuclei. More-direct evidence is scarce. In the lateral hypothalamus, exogenous CB_1 receptor stimulation inhibits orexinergic neurons by reducing the excitatory drive on them (Huang et al., 2007). In contrast, CB_1 receptor block attenuates orexin-A-induced feeding (Crespo et al., 2008). It was proposed that CB_1 and OX_1 receptors form heteromeric complexes, which may enhance orexin signaling (Hilairet et al., 2003; Ellis et al., 2006; Ward et al., 2011).

We showed previously that OX_1 orexin receptor activation strongly stimulates ^3H overflow from [^3H]AA-labeled cells (Turunen et al., 2010a). The full sensitivity of the response to the reputed phospholipase A_2 (PLA_2) inhibitor methyl arachidonyl fluorophosphonate (MAFP), in addition to partial sensitivity to inhibitors of other enzymes and intracellular signal pathways (Turunen et al., 2010a), suggests that this effect is mediated by PLA_2 enzymes. Although MAFP is very commonly used as a PLA_2 inhibitor, it is an analog of AA and is able to inhibit a number of serine hydrolases that hydrolyze ester- or amide-bound AA (De Petrocellis et al., 1997; Deutsch et al., 1997; Dinh et al., 2002; Savinainen et al., 2010). Therefore, does the ^3H overflow observed take place solely through PLA_2, and which isoform is involved? Another question left open is whether the ^3H overflow is composed only of AA or whether other water-soluble and secreted metabolites are involved. In the current study, we set out to resolve these questions. The results demonstrate that both free AA and AA incorporated into the endocannabinoid 2-AG are released upon orexin receptor stimulation. Both AA and 2-AG are shown to have signaling roles of their own.

Materials and Methods

Drugs. Human orexin-A and -B were obtained from NeoMPS (Strasbourg, France). 1-(2,4-Dichlorophenyl)-5-(4-iodophenyl)-4-methyl-*N*-1-piperidinyl-1*H*-pyrazole-3-carboxamide (AM-251), [4-[5-methoxy-2-oxo-1,3,4-oxadiazol-3(2*H*)-yl]-2-methylphenyl]carbamic acid phenylmethyl ester (CAY10499), *N*-[2-[4-(5-chloro-2,3-dihydro-2-oxo-1*H*-benzimidazol-1-yl)-1-piperidinyl]-1-methylethyl]-2-naphthalenecarboxamide (CAY10593) (compound 69 in Scott et al., 2009), *N*-cyclohexanecarbonylpentadecylamine (CCPA) (compound 17 in Tsuboi et al., 2004), 1,1,1,2,2-pentafluoro-7-phenyl-heptan-3-one (FKGK11) (compound 10a in Baskakis et al., 2008), 3-(1,1′-dimethylheptyl)-6*aR*,7,10,10*aR*-tetrahydro-1-hydroxy-6,6-dimethyl-6*H*-dibenzo[*b*,*d*]pyran-9-methanol (HU-210), 4-nitrophenyl-4-[dibenzo[*d*][1,3]dioxol-5-yl(hydroxy)methyl-]piperidine-1-carboxylate (JZL184), lipid standards (2-AG and AA), MAFP, pyrrophenone [*N*-[[(2*S*,4*R*)-1-[2-(2,4-difluorobenzoyl)benzoyl]-4-[(triphenylmethyl)thio]-2-pyrrolidinyl]methyl]-4-[(*Z*)-(2,4-dioxo-5-thiazolidinylidene)methyl]benzamide] (compound 6 in Seno et al., 2001), and [3-(3-carbamoylphenyl)phenyl] *N*-cyclohexylcarbamate (URB597) were obtained from Cayman Europe (Tallinn, Estonia). 1,6-Bis(cyclohexyloximinocarbonylamino) hexane (RHC-80267), 1-[2-methylbenzoxazol-6-yl]-3-[1,5] naphthyridin-4-yl-urea HCl (SB-334867), tetrahydrolipstatin (THL) (*N*-formyl-L-leucine-(1*S*)-1-[[(2*S*,3*S*)-3-hexyl-4-oxo-2-oxetanyl]methyl]dodecyl ester), and 1-[6-([(17*b*)-3-methoxyestra-1,3,5(10)-trien-17-yl]amino)hexyl]-1*H*-pyrrole-2,5-dione (U-73122) were obtained from Tocris Bioscience (Bristol, UK), fura-2 acetoxymethyl ester from Invitrogen (Carlsbad, CA), and [5,6,8,9,11,12,14,15-^3H]AA, [1-^{14}C]AA, and [9,10-^3H]oleic acid from PerkinElmer Life and Analytical Sciences (Waltham, MA). Forskolin, probenecid [*p*-(dipropylsulfamoyl)benzoic acid], and 3-isobutyl-1-methylxanthine (IBMX) were obtained from Sigma-Aldrich (St. Louis, MO).

Cell Culture. CHO-hOX_1 cells expressing ~500 fmol/mg of protein levels of high-affinity human OX_1 receptors (as determined from high-affinity ^{125}I-orexin-A binding (P. M. Turunen and J. P. Kukkonen, unpublished data) were described previously, as were their culture conditions (Lund et al., 2000; Turunen et al., 2010a). CHO-hCB_1 cells expressing human CB_{1a} receptors (Grimsey et al., 2010) were a kind gift from Dr. Michelle Glass (University of Auckland, Auckland, New Zealand) via Drs. Jarmo Laitinen and Juha Savinainen (University of Eastern Finland, Kuopio, Finland); these cells were propagated under the same conditions as CHO-hOX1 cells except that 0.25 mg/ml phleomycin (Zeocin; Invitrogen) was included. Neuro-2a-hOX_1, PC12-hOX_1, and wild-type HEK-293 cells were propagated as described previously (Holmqvist et al., 2002; Putula and Kukkonen, 2012) except that PC12 cells received an additional supplement of 5% horse serum (Invitrogen). For the ^3H overflow experiments with [^3H]AA- and [^3H]oleic acid-labeled cells and for the 2-AG reporter assays, the CHO-hOX_1 cells were cultivated on 24-well plates (well bottom area, 1.77 cm^2; Greiner Bio-One GmbH, Frickenhausen, Germany) coated with polyethylenimine (25 μg/ml for 1 h at 37°C; Sigma-Aldrich); for Ca^{2+} imaging, the cells were cultivated on polyethylenimine-coated, circular, glass coverslips (diameter, 13 mm; Menzel-Gläser, Braunschweig, Germany). For the thin-layer chromatography (TLC) assays, the cells were cultured on six-well plates (bottom area, 9.6 cm^2; Greiner Bio-One). For cAMP measurements (direct CB_1 receptor assay or 2-AG reporter assay), CHO-hCB_1 cells were cultured on plastic culture dishes (bottom area, 56 cm^2; Greiner Bio-One). HEK-293 cells were transiently transfected with hOX_1 receptor cDNA by using Fugene HD (Roche Diagnostics GmbH, Mannheim, Germany), as described previously (Putula and Kukkonen, 2012).

^3H Overflow from [^3H]AA- or [^3H]Oleic Acid-Labeled Cells. The experiments were largely performed as described previously (Turunen et al., 2010a). CHO-hOX_1 cells were plated on 24-well plates (20,000 cells per well) and left to grow for 24 h. The wells were precoated with polyethylenimine, which very much reduced cell detachment during the washes. Then, 0.1 μCi of [^3H]AA (or 0.2 μCi of [^3H]oleic acid, to compensate for the lower release levels and lower ^3H content) was added to each well, and the cells were cultured for another 20 h. The incubation medium was removed, the cells were washed twice with HEPES-buffered medium (HBM) (137 mM NaCl,

5 mM KCl, 1 mM $CaCl_2$, 1.2 mM $MgCl_2$, 0.44 mM KH_2PO_4, 4.2 mM $NaHCO_3$, 10 mM glucose, and 20 mM HEPES, adjusted to pH 7.4 with NaOH) supplemented with 2.4 mg/ml stripped bovine serum albumin (S-BSA) (Turunen et al., 2010b), and the cells were left in HBM with S-BSA at 37°C. The cells were immediately stimulated with orexin-A or thapsigargin for 7 min, after which 200 μl of the total volume of 250 μl in each well was transferred to Eppendorf tubes (VWR International, Radnor, PA) on ice. The samples were centrifuged (16,000*g* for 1.5 min at 4°C), 100 μl of the medium was transferred to a scintillation tube, scintillation cocktail (HiSafe 3; PerkinElmer Life and Analytical Sciences) was added, and the radioactivity was measured with a Wallac 1414 liquid scintillation counter (PerkinElmer Life and Analytical Sciences). It should be noted that total radioactivity released in the supernatant from the ^{3}H-preloaded cells was measured in this assay without any separation with respect to molecular species.

In some cases, orexin stimulation was preceded by some inhibitor preincubation. In such cases, the inhibitor used was added to the cells after one wash with HBM plus S-BSA, and the cells were preincubated for 30 min in HBM in the absence of S-BSA. HBM plus 10× S-BSA was added to a final concentration of S-BSA of 2.4 mg/ml for the last 5 min, to chelate the radioactivity leaked during this period. The incubation solution was removed, fresh HBM plus S-BSA with the inhibitor was added, and the cells were stimulated immediately with orexin-A for 7 min. The control cells were treated in the same way. The procedure effectively removed the radioactivity leaked during the preincubation period, and the S-BSA did not interfere with inhibitor entry into the cells.

Lipid Extraction and TLC. CHO-hOX_1, neuro-2A-hOX_1, PC12-hOX_1, or transiently hOX_1-transfected HEK-293 cells grown on six-well plates were labeled with [^{14}C]AA (0.2 μCi/ml) in cell culture medium (Ham's F12 medium) 16 h before the experiments. [^{14}C]AA loading medium was removed, and the cells were washed twice with HBM plus S-BSA (2.4 mg/ml) and stimulated with orexin-A for 7 min. Supernatants from the cells were rapidly removed and centrifuged (16,000*g* for 2 min at 4°C) to remove detached cells. The lipids were extracted from the supernatant with a slight modification of the method described by Bligh and Dyer (1959). Briefly, 800 μl of the total supernatant (1000 μl) was transferred to a Kimax tube (Kimble Glass, Inc., Vineland, NJ), 2 ml of methanol was added, followed by 1 ml of chloroform, and the tubes were shaken thoroughly. After the addition of 1 ml of water and 1 ml of chloroform, the tubes were shaken again and centrifuged (500*g* for 5 min at room temperature). The lower phase was collected and dried under a stream of N_2. The dried lipids were dissolved in chloroform, and the samples were applied to TLC plates (Silicagel 60; Merck, Darmstadt, Germany), which were dried at 110°C for 1 h. The plates underwent development with ethyl acetate/methanol (90:10) (Glass et al., 2005) in a chromatography tank lined with filter paper. Nonlabeled lipid standards were included on each TLC plate, either in separate lanes or together with the samples; the movement of the lipids of interest (2-AG and AA) in the samples was not affected by the presence of the standards. The average retardation factor values for AA and 2-AG were 0.58 ± 0.01 and 0.67 ± 0.01, respectively.

TLC data were quantitated both through imaging plate analysis and through scraping and scintillation counting; the two methods yielded comparable results (Jäntti et al., 2012). For this reason, only the results from the imaging plate analysis are presented. After development, the plates were vacuum-dried and an imaging plate (BAS-MS; Fujifilm, Tokyo, Japan) was exposed overnight. The imaging plate was scanned with a Fujifilm FLA 5100 scanner, and the band areas and intensities were measured with ImageJ (http://rsbweb.nih.gov/ij). The plate background was subtracted from the band intensities.

2-AG Reporter Assay and cAMP Measurements. 2-AG release from CHO-hOX_1 cells upon orexin receptor stimulation was detected and quantitated by using CHO-hCB_1 cells as detector cells; the assay is conceptually reminiscent of, for instance, a nitric oxide production assay (Hu and el-Fakahany, 1993). CHO-hCB_1 cells on cell culture dishes were prelabeled with 5 μCi/ml [^{3}H]adenine in culture medium for 2 h, after which the cells were washed with phosphate-buffered saline and detached with phosphate-buffered saline plus 0.2% (w/v) EDTA. The cells were centrifuged, resuspended in HBM containing 500 μM IBMX (a cyclic nucleotide phosphodiesterase inhibitor), and dispensed on top of CHO-hOX_1 cells growing on 24-well plates that had been washed with HBM. Different densities of CHO-hCB_1 cells were tested, but we finally chose a density of 150,000 cells per well. The plates were gently centrifuged (100*g* for 3 min at room temperature) to sediment CHO-hCB_1 cells on top of CHO-hOX_1 cells in HBM. The cells were allowed to rest at 37°C for 10 min, after which they were stimulated for 7 min with orexin-A or HU-210. The final volume in each well was 250 μl. When inhibitors were included, these cells (and the control cells) were preincubated with the inhibitor or vehicle for 10 min (SB-334867 and AM-251) or 30 min (THL) before orexin stimulation. The reactions were interrupted through rapid removal of the medium, addition of 300 μl of ice-cold 0.33 M perchloric acid, and freezing. The insoluble fragments of the thawed samples were centrifuged (1100*g* for 10 min at room temperature), and the [^{3}H]ATP/[^{3}H]ADP and [^{3}H]cAMP fractions of the cell extracts were isolated through sequential Dowex/alumina chromatography (Holmqvist et al., 2005). Radioactivity was determined by using scintillation counting; the conversion of [^{3}H]ATP to [^{3}H]cAMP was calculated as a percentage of the total eluted [^{3}H]ATP plus [^{3}H]ADP. Because only CHO-hCB_1 cells were prelabeled with [^{3}H]adenine, the radioactivity isolated was derived from those cells alone.

CHO-hCB_1 cells were also subjected to cAMP measurements in the absence of CHO-hOX_1 cells. The assay was similar to that described above, except that the detached cells were preincubated for 10 min in HBM plus IBMX (with inhibitors, if they were used) and then dispensed on 96-well plates (10^5 cells per well) where the stimulants (orexin-A, HU-210, and 2-AG) were already present. The final volume was 150 μl per well. On the plates, 0.5 mg/ml S-BSA was included, because this helped to maintain 2-AG in solution (Savinainen et al., 2003). After 10 min of stimulation, the reactions were interrupted through rapid centrifugation (1100*g* for 3 min at 4°C) of the cells, removal of the medium, addition of 150 μl of ice-cold 0.33 M perchloric acid, and freezing. The samples were then treated as described above.

Ca^{2+} Measurements. Cells plated on polyethylenimine-coated glass coverslips were loaded for 20 min at 37°C with 4 μM fura-2

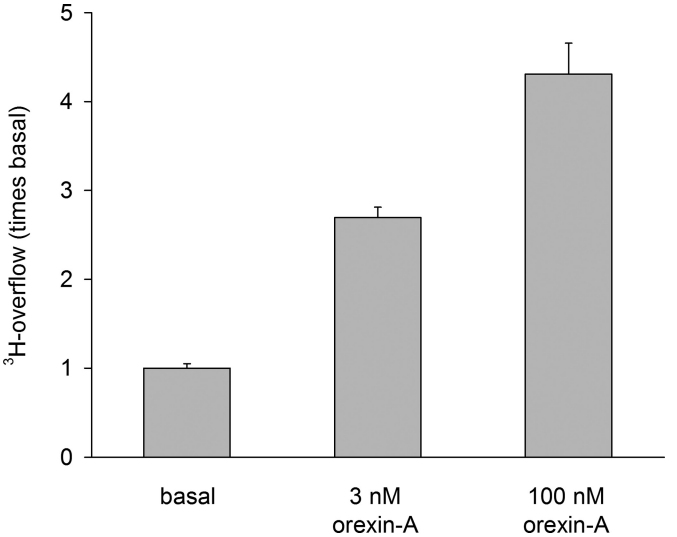

Fig. 1. Orexin-A-stimulated ^{3}H overflow from [^{3}H]AA-labeled CHO-hOX_1 cells.

acetoxymethyl ester in HBM containing 1 mM probenecid, rinsed once, and used immediately. Ca^{2+} measurements were performed at 35°C with a Nikon TE2000 fluorescence microscope (20×/0.75 air objective) and an Andor iXon 885 electron-multiplying charge-coupled device camera under the control of Nikon NIS Elements AR software with 6D extension (Nikon, Tokyo, Japan). For Ca^{2+} imaging, the cells were excited with alternating 340- and 380-nm light (Sutter DG4 Plus wavelength switcher; Sutter Instrument Company, Novato, CA), and the emitted light was collected through a 400-nm dichroic mirror and a 450-nm long-pass filter. Additions were made with constant perfusion (HBM with probenecid). When the inhibitors THL and pyrrophenone were tested, the cells were pretreated with the compounds for 20 min and the compounds were included in the perfusion medium throughout the experiment. Regions of interest were defined with NIS software, and the data were extracted to Microsoft Excel (Microsoft, Redmond, WA) for observation and quantitation. More than 30 cells were measured in each experiment, and each experiment was repeated four times or more.

Data Analysis. All data are presented as mean ± S.E.M.; N refers to the number of batches of cells. Each experiment was performed at least three times. The AA-release experiments were performed with six data points in parallel, imaging with 30 or more, cAMP measurements with three or four, and TLC with two. Student's two-tailed t test with Bonferroni correction was used for all pairwise comparisons except in Fig. 8, where, because of the nonparametric nature of cell counting, the χ^2 test also was used (Ekholm et al., 2007). Microsoft Excel was used for nonlinear curve-fitting for the determination of EC_{50} values. The effects of inhibitors on orexin-stimulated AA and 2-AG release were calculated from the values by using a formula that compensated for the possible effects of the inhibitors on basal release, i.e., release [percentage of

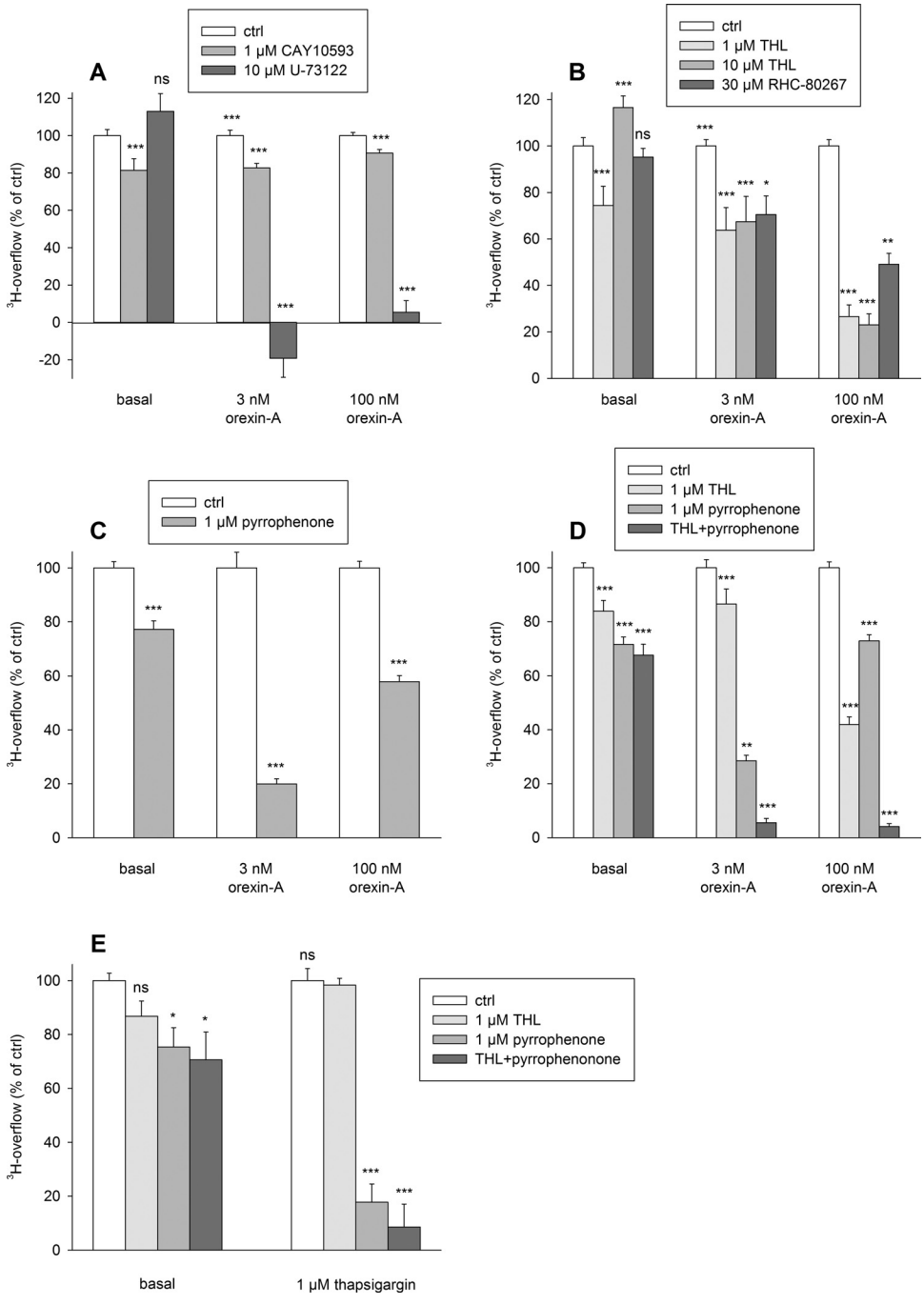

Fig. 2. Molecular mechanism of orexin-A and thapsigargin-stimulated ^{3}H overflow from [^{3}H]AA-labeled CHO-hOX_1 cells. A, the orexin response is inhibited by the PLC inhibitor U-73122 but not by the PLD1 inhibitor CAY10593. B and C, the orexin response is partially inhibited by the DAGL inhibitors THL and RHC-80267 (B) and the cPL$A_2\alpha/\zeta$ inhibitor pyrrophenone (C). D, the combination of THL and pyrrophenone produces full inhibition of the orexin response. E, the response to 1 μM thapsigargin is nearly fully blocked by pyrrophenone alone. The data were normalized so that each control response (basal, 3 nM orexin-A, and 100 nM orexin-A) amounts to 100% (see *Materials and Methods*). Some differences in the inhibitory efficacy can be seen in B, C, and D, because only experiments in which all of the inhibitors were tested were included in the analysis in D, to allow direct comparison of the efficacy of THL and pyrrophenone. Comparisons are to the corresponding control (ctrl) values (N = 3–7); ns, not significant ($p > 0.05$); *, $p < 0.05$; **, $p < 0.01$; ***, $p < 0.001$.

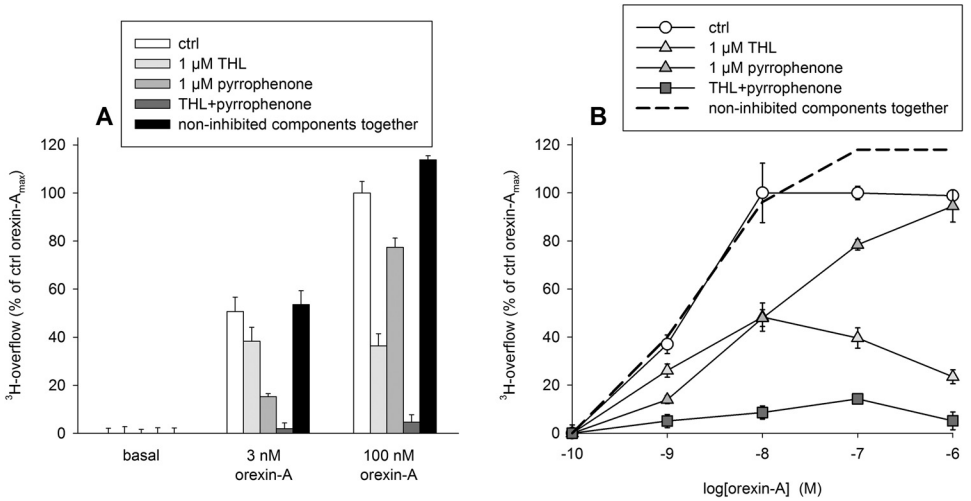

Fig. 3. Normalized raw data on the effects of the DAGL inhibitor THL and the $cPLA_2$ inhibitor pyrrophenone on the ^3H overflow from [^3H]AA-labeled CHO-hOX_1 cells. A, summarized data (same as in Fig. 2D; $N = 5$). The significances are the same as in Fig. 2D. B, representative experiment. The data were normalized so that each basal level is 0% and the maximal response to 100 nM orexin-A in the absence of inhibitors is 100% [response = ($orexin_{inhibitor}$ − $basal_{inhibitor}$)/($orexin_{100\ nM\text{-}ctrl}$ − $basal_{ctrl}$) × 100%]. ctrl, control; non-inhibited components together, procedure in which the orexin responses remaining after THL and pyrrophenone were added together.

control (noninhibited)] = ($orexin_{inhibitor}$ − $basal_{inhibitor}$)/($orexin_{control}$ − $basal_{control}$) × 100% (see Figs. 2 and 4). In this manner, the nontreated control values (basal, 1 nM orexin-A, and 100 nM orexin-A) are set to 100% and full inhibition to 0%.

Results

Orexin Receptor Stimulation Induces [^{3}H]AA-Derived ^{3}H Overflow through Distinct Cytosolic PLA_2 and Diacylglycerol Lipase Cascades. Our previous studies showed strong release of radioactivity from [^{3}H]AA-labeled CHO-hOX_1 cells upon OX_1 receptor stimulation (Fig. 1), but the enzymes responsible for this could not be resolved because of the low selectivity of the inhibitors available (Turunen et al., 2010a). We showed that OX_1 receptors also potently activate both phospholipase C (PLC) and phospholipase D (PLD) cascades (Johansson et al., 2008; Jäntti et al., 2012), producing diacylglycerol (DAG) and phosphatidic acid (PA), respectively. Both of these compounds could act as substrates for AA release, through the DAG lipase (DAGL)-monoacylglycerol lipase (MAGL) and PA-PLA_2 cascades, respectively, and PA can also be hydrolyzed to DAG by PA phosphohydrolase (reviewed in Kukkonen, 2011). Only PLD1 and not PLD2 is activated by orexin receptor stimulation in CHO cells, and this isoform can be fully inhibited by CAY10593 (Jäntti et al., 2012). CAY10593 produced very weak (10–20%) inhibition of ^{3}H overflow (Fig. 2A). In contrast, the PLC inhibitor U-73122 produced full inhibition (Fig. 2A).

THL is used as a pancreatic triglyceride lipase inhibitor, but it is an even more-potent inhibitor of some related enzymes, including DAGL (Lee et al., 1995; Bisogno et al., 2003), and it can be used at 1 μM as a relatively selective DAGL inhibitor (Bisogno et al., 2006) (V. Di Marzo, personal communication). THL produced significant inhibition of the orexin response even at 1 μM (Fig. 2B). RHC-80267, a less-potent DAGL inhibitor, showed a similar trend of inhibition (Fig. 2B).

Selective inhibitors for particular PLA_2 isoforms have been produced during the past 10 years. The most well characterized (e.g., for selectivity) of these are different pyrrolidine inhibitors for cytosolic PLA_2 ($cPLA_2$) α (Seno et al., 2000, 2001). A commercially available inhibitor of this type, pyrrophenone (Seno et al., 2001), at 1 μM produced significant inhibition of the orexin response (Fig. 2C). Interestingly, the inhibition profile was the opposite of that for THL; whereas THL apparently produced weaker inhibition with 3 nM orexin-A and stronger inhibition with 100 nM, pyrrophenone was stronger with 3 nM orexin-A. We hypothesized that DAGL and $cPLA_2$ might represent two components of the orexin-stimulated ^{3}H overflow from [^{3}H]AA-labeled cells. The combination of THL and pyrrophenone produced full inhibition of the orexin-A response (Fig. 2D). In contrast, the response to thapsigargin showed no sensitivity to THL but was almost fully inhibited by pyrrophenone alone (Fig. 2E), in agreement with Ca^{2+} activation of $cPLA_2$ (reviewed in Ghosh et al., 2006). Although Ca^{2+} level elevation should also stimulate DAGL (Bisogno et al., 2003), Ca^{2+} level elevation (at least when triggered by thapsigargin or ionomycin) is a poor stimulant of PLD and an even poorer stimulant of PLC in CHO cells (Lund et al., 2000; Johansson et al., 2007; Jäntti et al., 2012); therefore, in the absence of DAG production, there was no DAGL activity.

The orexin response appears to rely on two different components. The relative contributions of the components might become clearer with normalized raw data instead of inhibi-

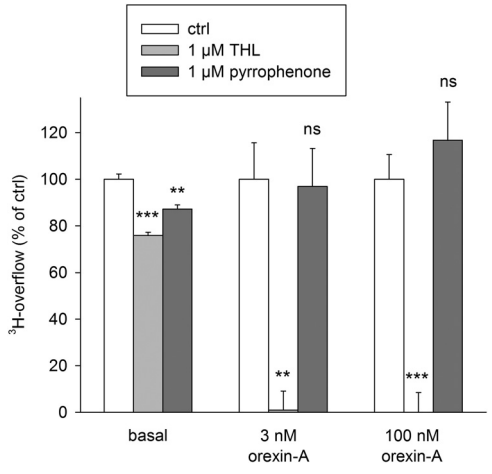

Fig. 4. Orexin-A-induced ^{3}H overflow from [^{3}H]oleic acid-labeled CHO-hOX_1 cells mediated by DAGL. Data were normalized as explained in *Materials and Methods* and for Fig. 2. Comparisons are to the corresponding control (ctrl) values ($N = 5$); ns, not significant ($p > 0.05$); **, $p < 0.01$; ***, $p < 0.001$.

tion data (Fig. 3A). The same finding could also be seen with more complete concentration-response curves (Fig. 3B). The patterns of inhibition with THL and pyrrophenone were essentially not overlapping (Fig. 3). In the analyses of the concentration-response data, the control pEC_{50} value was 8.7 ± 0.1 and the pEC_{50} values after pyrrophenone (putative DAGL component) and THL (putative $cPLA_2$ component) treatment were 8.4 ± 0.1 and 9.3 ± 0.1, respectively (N = 3–5). Therefore, the putative $cPLA_2$ component would be activated with significantly higher potency (see *Discussion*).

We showed previously that ^3H overflow from [^3H]oleic acid-labeled cells was stimulated by OX_1 receptor activation in CHO-hOX_1 cells, although with significantly lower potency and efficacy than in [^3H]AA-labeled cells (Turunen et al., 2010a). The potency of this ^3H overflow seemed to overlap better with the DAGL component of AA release than with AA release in its entirety. Orexin-induced ^3H overflow from [^3H]oleic acid-labeled cells was inhibited fully by THL but not at all by pyrrophenone (Fig. 4). [^3H]Oleic acid is likely to end up in the *sn1* position, which is not hydrolyzed by $cPLA_2$. Even if some oleic acid would be found in the *sn2* position, $cPLA_2\alpha$ (in contrast to other PLA_2 isoforms, including $cPLA_2\zeta$) is rather specific for AA in the *sn2* position (reviewed in Ghosh et al., 2006, 2007).

Endocannabinoid-Hydrolyzing Enzymes, Hormone-Sensitive Lipase, and Intracellular PLA_2 in Orexin-Induced, AA-Derived ^3H Overflow. DAG lipases are thought to show *sn1* selectivity (3–8-fold in vitro) (Bisogno et al., 2003); therefore, DAGL might be thought to be unlikely to release AA from its usual *sn2* position. DAGL, however, works as a "gatekeeper" for MAGL, because no monoacylglycerol should be produced in the absence of DAGL activity. We tested a selective MAGL inhibitor, JZL184 (Long et al., 2009). JZL184 (10 μM) produced weak but significant inhibition ($20 \pm 12\%$ with 3 nM orexin-A, $p < 0.01$; $11 \pm 10\%$ with 100 nM orexin-A, $p < 0.05$) (Supplemental Fig. 1). We similarly tested inhibitors of fatty acid amide-type endocannabinoid-hydrolyzing enzymes, URB597 (100 nM; fatty acid

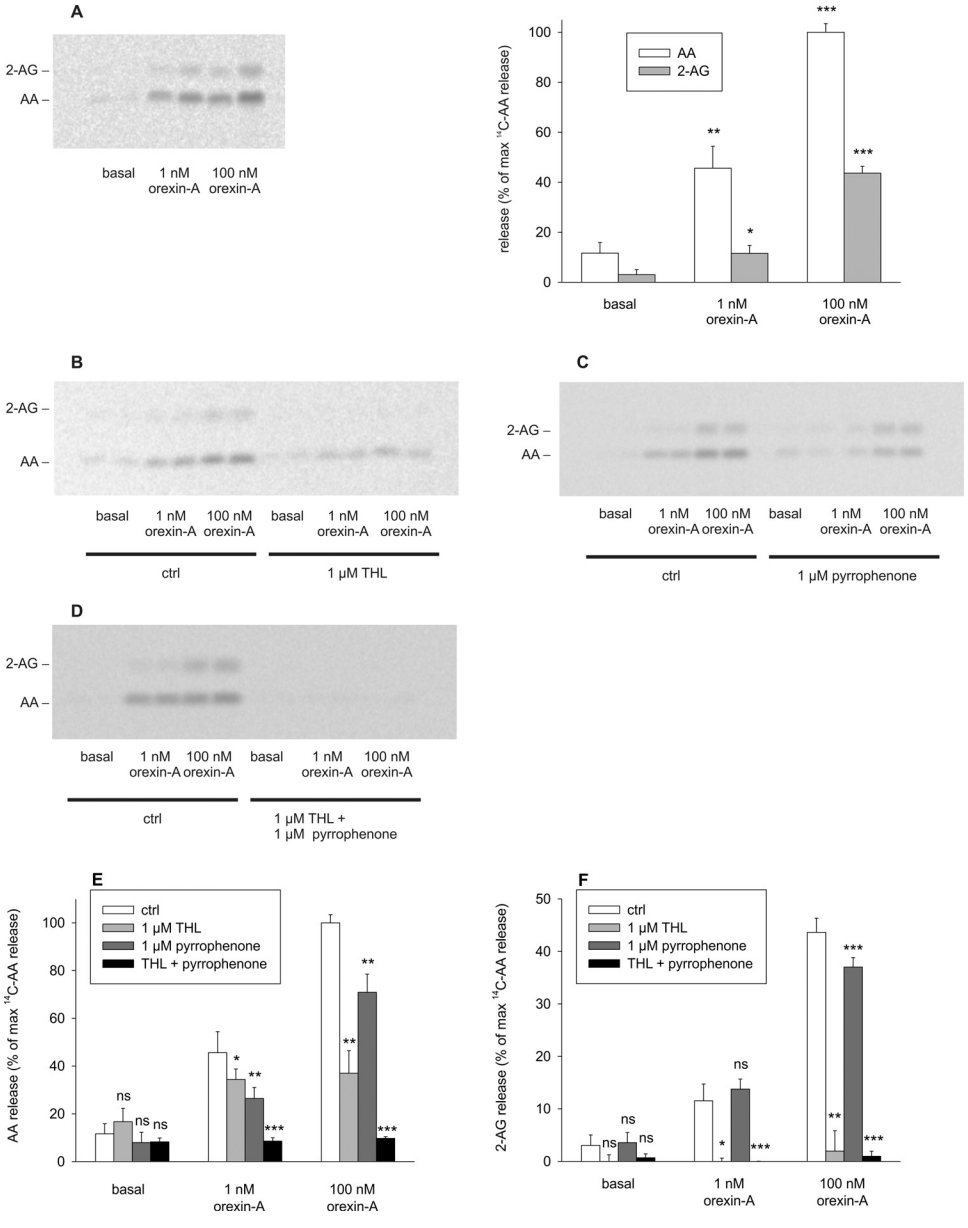

Fig. 5. TLC separation of the [^{14}C]AA-labeled lipid species released from CHO-hOX_1 cells. A, release of both free AA and 2-AG upon orexin stimulation (N = 8). B, inhibitory actions of THL. C, inhibitory actions of pyrrophenone. D, combined effects of THL and pyrrophenone on AA and 2-AG release upon OX_1 receptor stimulation. E, summarized data for inhibition of AA release (N = 3–5). F, summarized data for inhibition of 2-AG release (N = 3–5). The data in the bar graphs were normalized to the AA-release response to 100 nM orexin-A (100%). Comparisons are to the corresponding control (ctrl) values; ns, not significant ($p > 0.05$); *, $p < 0.05$; **, $p < 0.01$; ***, $p < 0.001$.

amide hydrolase [FAAH] inhibitor) and CCPA (100 μM; *N*-acylethanolamine-hydrolyzing acid amidase/acidic palmitoyl ethanolamidase inhibitor) (Kathuria et al., 2003; Tsuboi et al., 2004; Long et al., 2009). Neither URB597 nor CCPA significantly inhibited orexin-induced ^{3}H overflow from [^{3}H]AA-labeled cells (Supplemental Fig. 1). Similarly, the hormone-sensitive lipase/FAAH/MAGL inhibitor CAY10499 (30 μM) and the intracellular PLA_2 ($iPLA_2$) inhibitor FKGK11 (10 μM) (Baskakis et al., 2008; Muccioli et al., 2008; Minkkilä et al., 2009) were incapable of inhibiting the orexin response (Supplemental Fig. 1).

^{3}H Overflow from [^{3}H]AA-Labeled Cells Consists of Free AA and the Endocannabinoid 2-AG. The ^{3}H overflow method used here is well established and is often used in AA-release studies. It does not indicate [^{3}H]AA release specifically, however, and indicates only that [^{3}H]AA-derived radioactivity is released from the cells. Therefore, we conducted TLC separation of the molecular species released; to allow use of imaging plate identification of multiple molecular species, the cells were labeled with [^{14}C]AA. The results showed that the radioactivity released upon orexin receptor stimulation was found both in free AA and in the endocannabinoid 2-AG (Fig. 5A); AA was released with significantly higher potency by $cPLA_2$ (AA release in the presence of THL) than was 2-AG by DAGL (pEC_{50} values of 9.8 $\pm$ 0.1 and 8.3 $\pm$ 0.1, respectively; N = 3–9) (Fig. 6). THL fully blocked orexin-stimulated 2-AG release but only partly reduced AA release (Figs. 5, B, E, and F, and 6). In contrast, pyrrophenone inhibited only AA and not 2-AG release (Fig. 5, C, E, and F). Inclusion of both THL and pyrrophenone fully inhibited orexin-stimulated release of both free AA and 2-AG (Fig. 5, D, E, and F).

Other OX_1 receptor-expressing cells showed distinct responses to orexin-A stimulation. Neuro-2a and HEK-293 cells showed strong 2-AG release with 100 nM orexin-A (Supplemental Fig. 2). In addition, AA release was seen; orexin stimulation of 2-AG and AA release was eliminated by THL (data not shown), which suggests that AA was released through 2-AG breakdown and not through PLA_2 action on phospholipids. PC12 cells showed high basal levels of AA release, with no apparent stimulation with orexin-A, and no 2-AG release (Supplemental Fig. 2).

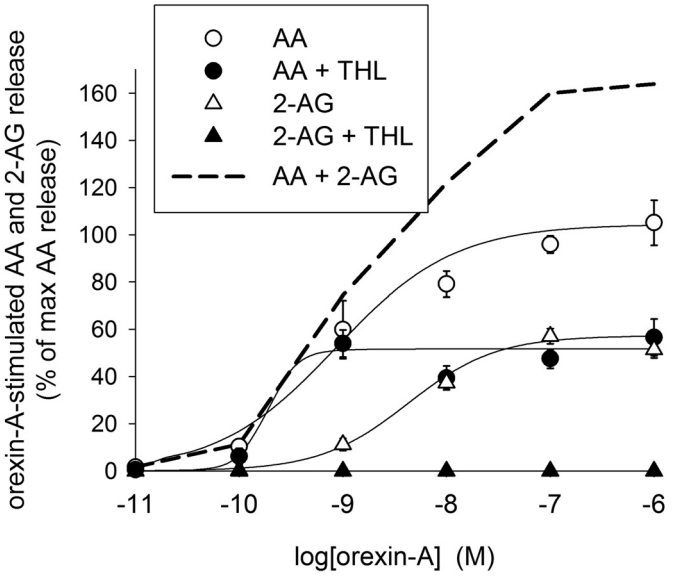

Fig. 6. Concentration-response curves for orexin-A with respect to [^{14}C]AA-labeled lipid species released from CHO-hOX_1 cells (as in Fig. 5). 2-AG release was fully blocked by THL (1 μM); therefore, data are not shown.

Orexin Receptor Activation Is Able to Induce Strong Paracrine Signaling to Cannabinoid Receptors through 2-AG. 2-AG is a potent endogenous ligand for cannabinoid receptors (reviewed in Di Marzo and Petrosino, 2007; Kano et al., 2009). Therefore, we tested whether 2-AG released upon orexin receptor signaling was able to activate cannabinoid receptors. For this, we designed a cell-cell communication assay between CHO-hOX_1 and CHO-hCB_1 cells, as described in *Materials and Methods*. CHO-hCB_1 cells were plated on top of the CHO-hOX_1 cell culture, CHO-hOX_1 cells were stimulated with orexin-A, and 2-AG production was detected as selective inhibition of adenylyl cyclase in CHO-hCB_1 cells. Orexin-A in this assay caused strong potent inhibition of adenylyl cyclase activity in CHO-hCB_1 cells, although the efficacy was somewhat lower than that of direct stimulation with the CB_1 agonist HU-210 (Fig. 7, A and B). The response to orexin-A was fully inhibited by the OX_1 receptor antagonist SB-334867, by THL, and by the CB_1 receptor antagonist/inverse agonist AM-251 (Fig. 7A), which indicated that inhibition of forskolin-stimulated adenylyl cyclase activity in CHO-hCB_1 cells by orexin-A was mediated through the cascade of orexin-A $\rightarrow$ OX_1 (on CHO-hOX_1 cells) $\rightarrow\rightarrow$ 2-AG (by DAGL in CHO-hOX_1 cells) $\rightarrow$ CB_1 (on CHO-hCB_1 cells). AM-251 but neither THL nor SB-334867 enhanced the forskolin-stimulated cAMP production (Fig. 7A), which suggests that CB_1 receptors show some constitutive activity. SB-334867 alone weakly inhibited the forskolin response (Fig. 7A), which suggests that SB-334867 shows some weak partial agonist activity at OX_1 receptors, in line with some previous observations (Bengtsson et al., 2007) (J. Putula and J. P. Kukkonen, unpublished observations). AM-251 at 10 μM strongly but incompletely inhibited the response to 1 μM HU-210 (data not shown; see also below).

In CHO-hCB_1 cells alone, exogenous 2-AG was nearly as efficacious as HU-210 as a CB_1 receptor activator (Fig. 7, C and D). AM-251 increased adenylyl cyclase activity, compared with forskolin alone (Fig. 7C), as also seen in the reporter assay (Fig. 7A), and fully blocked the response to 2-AG (Fig. 7C). In contrast, the response to 1 μM HU-210 was not fully blocked (data not shown), similar to the reporter assay results, which likely reflects the fact that the affinity/potency of HU-210 is too high (~100–1000-fold higher than that of 2-AG) to be fully blocked at this concentration by 10 μM AM-251.

To obtain an estimate of the 2-AG levels reached upon orexin receptor stimulation, we measured the potency of exogenous 2-AG to activate CB_1 receptors in CHO-hCB_1 cells (Fig. 7D). With the use of these data (maximal inhibition = 86 $\pm$ 3%, pEC_{50} = 7.40 $\pm$ 0.03, n_H = 1.1 $\pm$ 0.2; N = 5) as a standard curve for calculation of 2-AG levels from data on adenylyl cyclase inhibition by orexin-A in the reporter assay (maximal inhibition = 60 $\pm$ 3%, pEC_{50} = 9.1 $\pm$ 0.1, n_H = 1.5 $\pm$ 0.1; N = 4), the average orexin-A-induced increase in 2-AG levels sensed by the CHO-hCB_1 cells may be ~87 nM and the pEC_{50} for orexin-A for 2-AG production ~8.8.

$cPLA_2$ but Not DAGL Activity Is Pivotal for OX_1 Receptor Activation of Receptor-Operated Ca^{2+} Influx. We showed previously that MAFP could strongly inhibit OX_1 receptor-operated Ca^{2+} influx (Turunen et al., 2010a), which is central for orexin receptor-mediated Ca^{2+} level increases

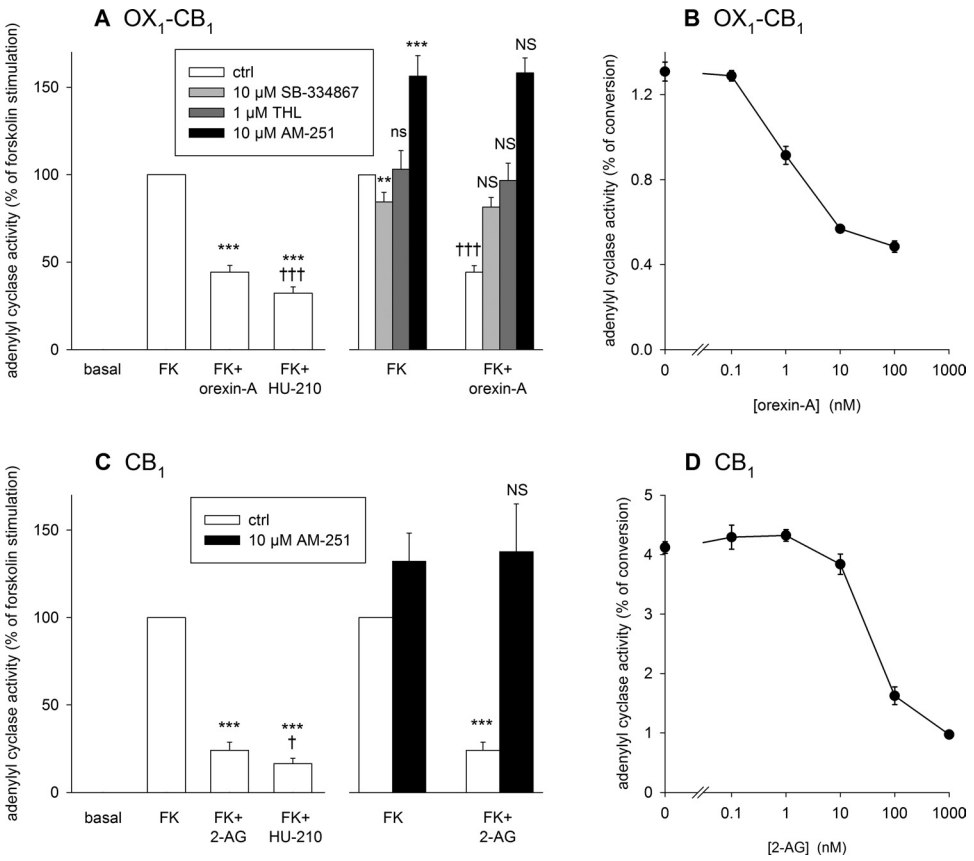

Fig. 7. OX_1-CB_1 receptor communication through OX_1 receptor-induced 2-AG production. A and B, OX_1-CB_1 communication assay; C and D, CHO-hCB_1 cells alone. A, summarized data for communication between OX_1 and CB_1 receptors ($N = 5$ or 6). The data were normalized to basal levels (0%) and control forskolin (FK) responses (100%). Left, adenylyl cyclase inhibition with 100 nM orexin-A and direct CB_1 receptor stimulation with 1 μM HU-210. Comparison to forskolin alone: ***, $p < 0.001$; comparison to forskolin plus orexin-A: †††, $p < 0.001$. Right, sensitivity of the orexin response to the OX_1 receptor antagonist SB-334867, the DAGL inhibitor THL, and the CB_1 receptor antagonist/inverse agonist AM-251. Comparison to forskolin alone: ns, not significant ($p > 0.05$); **, $p < 0.01$; ***, $p < 0.001$; comparison to forskolin in the presence of inhibitor (forskolin plus SB-334867 for forskolin plus SB-334867 plus orexin-A, forskolin plus THL for forskolin plus THL plus orexin-A, and forskolin plus AM-251 for forskolin plus AM-251 plus orexin-A): NS, not significant ($p > 0.05$); †††, $p < 0.001$. B, concentration-response curve for orexin-A in OX_1-CB_1 communication assay (representative data from a single experiment). C, CB_1 receptor responses in CHO-hCB_1 cells alone (summarized data; $N = 4–6$). The data were normalized as in A. Left, direct stimulation of CB_1 receptors with 1 μM 2-AG or 1 μM HU-210. Comparison to forskolin alone: ***, $p < 0.001$; comparison to forskolin plus 2-AG: †, $p < 0.05$. Right, sensitivity of the 2-AG response to the CB_1 receptor antagonist/inverse agonist AM-251. Comparison to forskolin alone: ***, $p < 0.001$; comparison to forskolin in the presence of AM-251: NS, not significant ($p > 0.05$). D, concentration-response curve for 2-AG (representative data from a single experiment).

because it also drives PLC activity at low orexin concentrations (Lund et al., 2000; Johansson et al., 2007). Because MAFP is a potent inhibitor of both the $cPLA_2$ and DAGL pathways, we tested selective inhibitors of these pathways, i.e., pyrrophenone and THL, in Ca^{2+} imaging assays. Pyrrophenone produced equally strong inhibition (Fig. 8, A and B), compared with MAFP (data not shown) (Turunen et al., 2010a), whereas THL was incapable of inhibiting the Ca^{2+} influx response (Fig. 8, A and C), which clearly indicates that the $cPLA_2$ pathway is involved in orexin receptor-operated Ca^{2+} influx. Inclusion of both pyrrophenone and THL did not produce stronger inhibition than that observed with pyrrophenone alone (Fig. 8, A, B, and D).

Discussion

We targeted the [^{3}H]AA-derived ^{3}H overflow by using a number of established or novel inhibitors of lipases and amidases that are capable of releasing AA. Most importantly, THL, an inhibitor of DAGL, and pyrrophenone, an inhibitor of $cPLA_2\alpha$ and -ζ (Seno et al., 2001; Ghomashchi et al., 2010) produced complementary inhibition, together reaching full inhibition. THL was selected as the DAGL inhibitor for detailed investigations because of its greater potency, efficacy, and stability and its likely greater selectivity, compared with RHC-80267. The pharmacological selectivity of the inhibitors in CHO cells was confirmed with respect to thapsigargin-induced ^{3}H overflow from [^{3}H]AA-labeled cells (fully inhibited by pyrrophenone) and orexin-A-induced ^{3}H overflow from [^{3}H]oleic acid-labeled cells (fully inhibited by THL). The conclusive evidence was obtained through TLC separation of [^{14}C]AA-labeled lipid species, which showed that the apparent orexin-A-induced AA overflow was composed of free AA as well as 2-AG. 2-AG release was fully dependent on DAGL (inhibited by THL), whereas the free AA component was dependent on both the $cPLA_2$ and DAGL pathways (additively inhibited by pyrrophenone and THL, respectively). The results are summarized in Fig. 9. The DAGL pathway is likely to follow from PLC activity, as suggested by both inhibition by the PLC inhibitor U-73122 and only minor inhibition by the PLD inhibitor CAY10593. 2-AG production closely mirrors PLC activity, as judged from total inositol phosphate release and DAG generation in the presence of

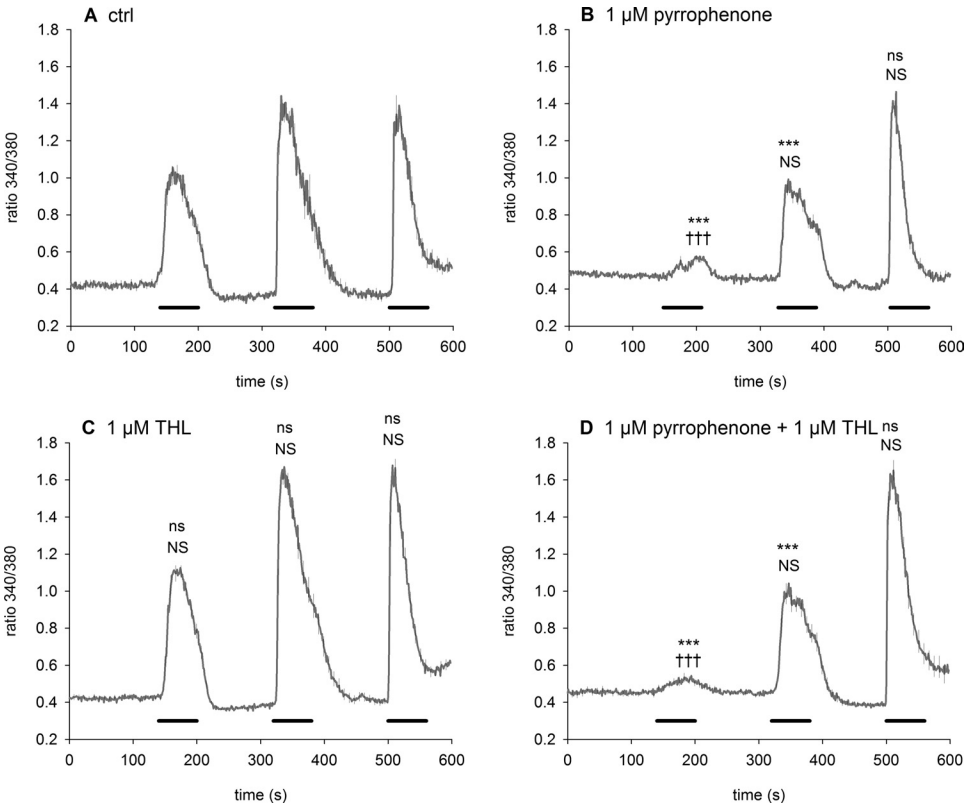

Fig. 8. Dependence on $cPLA_2$ of the Ca^{2+} signaling of orexin receptors. A, control CHO-hOX_1 cells. B, cells pretreated with and assayed in the presence of 1 μM pyrrophenone. C, cells pretreated with and assayed in the presence of 1 μM THL. D, cells pretreated with and assayed in the presence of both 1 μM pyrrophenone and 1 μM THL. Each panel is a representative average trace from one coverslip with 31 to 53 cells. S.E. values are shown only for every eighth point, for the sake of clarity. Black bars under the traces, successive additions of 0.3, 3, and 30 nM orexin-A. Comparison to control, maximal response (t test): ns, not significant ($p > 0.05$); ***, $p < 0.001$; number of cells responding (χ^2 test): NS, not significant ($p > 0.05$); †††, $p < 0.001$.

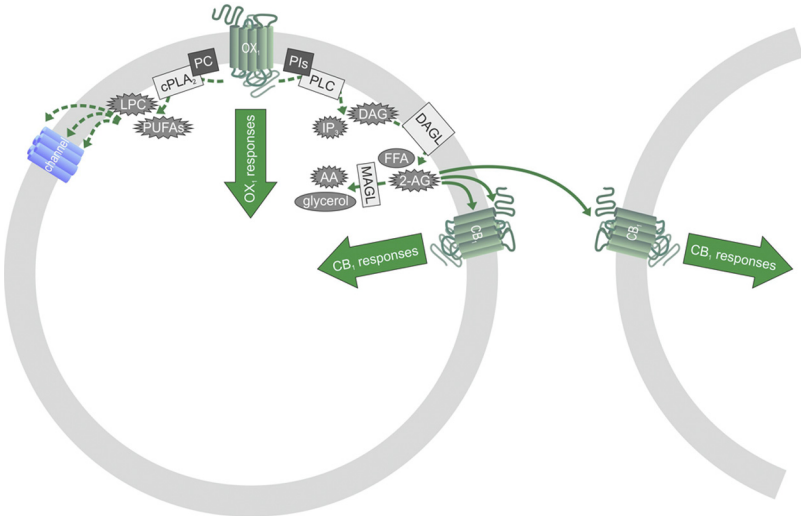

Fig. 9. Signaling scheme based on the results and suggestions of the present study. Orexin receptor stimulation leads to activation of both PLC (PLCβ?)-DAGL and $cPLA_2$ cascades. The former produces the endocannabinoid 2-AG, which is able to act either from the membrane face or from the extracellular side on CB_1 receptors expressed in the same cells. The CB_1 receptor-dependent and other OX_1-triggered signal cascades may interact within the cell. 2-AG may also exit the cells and stimulate CB_1 receptors on nearby cells. The other products of DAGL activity, mainly saturated free fatty acids (FFA), may not have important signaling roles. $cPLA_2$ likely acts on phosphatidylcholine (PC), leading to production of lysophosphatidylcholine (LPC) and polyunsaturated fatty acids (PUFAs) such as AA. Either lysophosphatidylcholine or polyunsaturated fatty acids or their metabolites centrally contribute to activation of the orexin receptor-operated Ca^{2+} influx channel. PIs, phosphatidylinositols; IP_3, inositol-1,4,5-trisphosphate.

PLD inhibition (Johansson et al., 2008). It is unclear, however, whether DAGL in general passively follows PLC activity or is actively regulated by, e.g., Ca^{2+} level elevation (Bisogno et al., 2003) or phosphorylation. MAGL or another component with similar activity (Long et al., 2009), degrading 2-AG to glycerol and AA, is likely to be responsible for the inhibition of free AA release by THL. We also used a number of other inhibitors of enzymes with possible AA-releasing capacity, including the MAGL inhibitor JZL184, the FAAH inhibitor URB597, the MAGL/FAAH/hormone-sensitive lipase inhibitor CAY10499, the $iPLA_2$ inhibitor FKGK11, and the *N*-acylethanolamine-hydrolyzing acid amidase/acidic palmitoyl ethanolamidase inhibitor CCPA. Whereas JZL184, URB597, and CAY10499 are rather well characterized, FKGK11 and CCPA are not (they have been used in only a few studies), and it was difficult to estimate their effective concentrations. However, none of the inhibitors except JZL184 produced any inhibition, which is logical in light of the studies clearly indicating the involvement of $cPLA_2$ and DAGL only. It is unclear why JZL184 produced a small but significant amount of inhibition of ^3H overflow. At the concentration used, CAY10499 also is an effective inhibitor of MAGL (Muccioli et al., 2008; Minkkilä et al., 2009), but it did not show any inhibition here; therefore, it is possible that the inhibition seen with JZL184 is attributable to an effect on some target other than MAGL.

$cPLA_2$ is activated with high potency by orexin receptors and may be a potent physiological signal. In the current study, we could verify that it was $cPLA_2$ and not DAGL signaling that was required for the activity of the receptor-operated Ca^{2+} influx pathway. Our results do not reveal,

however, whether it is AA or some other polyunsaturated fatty acid, the other product of $cPLA_2$ activity, lysophosphatidylcholine, or some metabolite of those compounds that mediates the response. All of those metabolites could be active at transient receptor potential or ARC channels (reviewed in Kukkonen, 2011).

$cPLA_2$ enzymes are known to be sensitive to Ca^{2+} level increases. The PLC inhibitor U-73122 fully inhibited ^3H overflow from [^3H]AA-labeled cells, which suggested that PLC activity was required for both $cPLA_2$ and DAGL pathways. U-73122 is known to be toxic to CHO cells (Taylor and Broad, 1998; Lund et al., 2000) and it can fully block orexin receptor-mediated Ca^{2+} influx (Smart et al., 1999), although inositol-1,4,5-trisphosphate-dependent Ca^{2+} influx is not involved in this response (Ekholm et al., 2007). In addition, $cPLA_2$ activity occurs with a higher potency than PLC or DAGL activity (see below). Therefore, we doubt the conclusion regarding involvement of PLC in $cPLA_2$ activation. Unfortunately, there are no other effective (and nontoxic) PLC inhibitors available (at least for CHO cells), and the activation mechanism for $cPLA_2$ thus remains unclear. However, we know that the increase in Ca^{2+} levels (likely through influx) induced by thapsigargin is a potent stimulator of $cPLA_2$ in these cells (present study) (Turunen et al., 2010a), and Ca^{2+} influx is required for effective stimulation of ^3H overflow from [^3H]AA-labeled cells by orexin-A (Turunen et al., 2010a). It is possible that there is a feed-forward cycle in orexin receptor signaling involving $cPLA_2$ and receptor-operated Ca^{2+} influx. However, additional experiments are required to resolve this and alternative options.

The potency of orexin-A for $cPLA_2$ and DAGL activation was determined in several ways. 2-AG would be released by DAGL with pEC_{50} values of 8.4 (^3H overflow in the presence of pyrrophenone), 8.3 (TLC assay), and 8.8 (2-AG release reporter assay). AA would be released by $cPLA_2$ with pEC_{50} values of 9.3 (^3H overflow in the presence of THL) and 9.8 (TLC assay in the presence of THL). Some of the variation may depend on the resolution of the assays; for example, TLC separation showed much less variation and thus greater sensitivity than the ^3H overflow assay. $cPLA_2$ was clearly activated with significantly greater potency than DAGL in CHO cells. In the other cell types examined, the situation was different. It is interesting that, in all of these cell types, orexin receptors couple to PLC (Holmqvist et al., 2002; Putula and Kukkonen, 2012); therefore, the differences in 2-AG release might be related to another component, such as lack of DAGL or the putative 2-AG transporter or effective alternative metabolism of DAG or degradation of 2-AG.

Our previous results obtained with the reputed $iPLA_2$ inhibitor bromoenol lactone suggested partial involvement of $iPLA_2$ in the orexin-stimulated ^3H overflow (Turunen et al., 2010a). Bromoenol lactone is known to act on different serine hydrolases (reviewed in Balsinde and Balboa, 2005), forming a soluble, reactive, molecular species that can form cysteine adducts with bystander proteins (Song et al., 2006). We are convinced that the previous results obtained with bromoenol lactone do not indicate the involvement of $iPLA_2$ but represent a result of nonspecific interactions of this inhibitor. This is supported by the fact that a novel $iPLA_2$ inhibitor, FKGK11, did not inhibit ^3H overflow.

Orexin-endocannabinoid interactions have been investigated in a few studies. CB_1 receptor mRNA and preproorexin mRNA are expressed in close apposition in the lateral hypothalamus, in part in the same cells (Cota et al., 2003). The physiological functions of orexins and endocannabinoids in appetite stimulation are similar, and leptin, a satiety messenger and negative regulator of orexinergic neurons (Håkansson et al., 1999; López et al., 2000), is also a negative regulator of endocannabinoid levels (Di Marzo et al., 2001). These systems may be involved in the same pathways. A study indicated endocannabinoid involvement in orexin-mediated stimulation of appetite (Crespo et al., 2008), and similar findings are indicated for the analgesic action of orexin-A (Ho et al., 2011). In contrast, endocannabinoids inhibit orexin signaling in the lateral hypothalamus by reducing the excitatory glutamatergic drive to orexinergic neurons (Huang et al., 2007). Endocannabinoids may have different functions in the lateral hypothalamus and in upstream regulatory centers of orexinergic neurons; whereas endocannabinoids in the lateral hypothalamus may suppress orexinergic neurons (Huang et al., 2007), endocannabinoids in the nucleus accumbens shell may stimulate activation of orexinergic neurons (Kirkham et al., 2002; Zheng et al., 2003; Soria-Gómez et al., 2007), and orexinergic projections to the nucleus accumbens shell (Mori et al., 2011) may cause a positive feedback cycle. The few studies performed suggested interactions between these systems, but the conclusions are not straightforward. Some of the problems arise from methodological obstacles, such as unreliable anti-orexin receptor antibodies (J. P. Kukkonen, unpublished data). In addition, the studies conducted were performed either with intact animals or with ex vivo slice preparations, where the neuronal circuitry involved may cause problems in identifying the actual sites of action of orexins and endocannabinoids.

In conclusion, the present study identified two enzyme cascades, $cPLA_2$ and DAGL, as potent orexin receptor targets and as the enzymes entirely responsible for the previously reported orexin-induced ^3H overflow from [^3H]AA-labeled cells (Turunen et al., 2010a). The activation mechanisms for either enzyme species remain unclear. Each enzyme activity produces a signal of its own. Although $cPLA_2$ appears essential for the receptor-operated Ca^{2+} influx, DAGL produces 2-AG, which is able to activate CB_1 cannabinoid receptors in a paracrine manner. This indicates that the suggested interactions between orexinergic and cannabinoidergic systems in the brain may take place through paracrine endocannabinoid signaling and that regulation of the some of the same physiological responses in appetite, for example, may take place through an arrangement such as this. Orexin receptors were suggested previously to heterodimerize with CB_1 receptors in heterologous coexpression systems (Hilairet et al., 2003; Ellis et al., 2006; Ward et al., 2011). Our view is that interactions (alternatively or additionally) take place through 2-AG production, which represents a much more flexible signal system that does not require any molecular interactions between orexin and endocannabinoid receptors.

Acknowledgments

We gratefully acknowledge Drs. Michelle Glass (University of Auckland, Auckland, New Zealand) and Jarmo Laitinen and Juha Savinainen (University of Eastern Finland, Kuopio, Finland) for the CHO-hCB_1 cells, Drs. Vincenzo Di Marzo (Institute of Biomolecular Chemistry, Consiglio Nazionale delle Ricerche, Pozzuoli, Italy) and

Jarmo Laitinen for advice on the experiments, and Pirjo Puroranta for technical assistance.

Authorship Contributions

Participated in research design: Turunen, Jäntti, and Kukkonen.
Conducted experiments: Turunen and Jäntti.
Contributed new reagents or analytic tools: Kukkonen.
Performed data analysis: Turunen, Jäntti, and Kukkonen.
Wrote or contributed to the writing of the manuscript: Turunen, Jäntti, and Kukkonen.

References

Balsinde J and Balboa MA (2005) Cellular regulation and proposed biological functions of group VIA calcium-independent phospholipase A_2 in activated cells. *Cell Signal* **17:**1052–1062.

Baskakis C, Magrioti V, Cotton N, Stephens D, Constantinou-Kokotou V, Dennis EA, and Kokotos G (2008) Synthesis of polyfluoro ketones for selective inhibition of human phospholipase A_2 enzymes. *J Med Chem* **51:**8027–8037.

Bengtsson MW, Mäkelä K, Sjöblom M, Uotila S, Akerman KE, Herzig KH, and Flemström G (2007) Food-induced expression of orexin receptors in rat duodenal mucosa regulates the bicarbonate secretory response to orexin-A. *Am J Physiol Gastrointest Liver Physiol* **293:**G501–G509.

Bisogno T, Cascio MG, Saha B, Mahadevan A, Urbani P, Minassi A, Appendino G, Saturnino C, Martin B, Razdan R, et al. (2006) Development of the first potent and specific inhibitors of endocannabinoid biosynthesis. *Biochim Biophys Acta* **1761:** 205–212.

Bisogno T, Howell F, Williams G, Minassi A, Cascio MG, Ligresti A, Matias I, Schiano-Moriello A, Paul P, Williams EJ, et al. (2003) Cloning of the first sn1-DAG lipases points to the spatial and temporal regulation of endocannabinoid signaling in the brain. *J Cell Biol* **163:**463–468.

Bligh EG and Dyer WJ (1959) A rapid method of total lipid extraction and purification. *Can J Biochem Physiol* **37:**911–917.

Cota D, Marsicano G, Tschöp M, Grübler Y, Flachskamm C, Schubert M, Auer D, Yassouridis A, Thöne-Reineke C, Ortmann S, et al. (2003) The endogenous cannabinoid system affects energy balance via central orexigenic drive and peripheral lipogenesis. *J Clin Invest* **112:**423–431.

Crespo I, Gómez de Heras R, Rodríguez de Fonseca F, and Navarro M (2008) Pretreatment with subeffective doses of Rimonabant attenuates orexigenic actions of orexin A-hypocretin 1. *Neuropharmacology* **54:**219–225.

De Petrocellis L, Melck D, Ueda N, Maurelli S, Kurahashi Y, Yamamoto S, Marino G, and Di Marzo V (1997) Novel inhibitors of brain, neuronal, and basophilic anandamide amidohydrolase. *Biochem Biophys Res Commun* **231:**82–88.

Deutsch DG, Omeir R, Arreaza G, Salehani D, Prestwich GD, Huang Z, and Howlett A (1997) Methyl arachidonyl fluorophosphonate: a potent irreversible inhibitor of anandamide amidase. *Biochem Pharmacol* **53:**255–260.

Di Marzo V, Goparaju SK, Wang L, Liu J, Bátkai S, Járai Z, Fezza F, Miura GI, Palmiter RD, Sugiura T, et al. (2001) Leptin-regulated endocannabinoids are involved in maintaining food intake. *Nature* **410:**822–825.

Di Marzo V and Petrosino S (2007) Endocannabinoids and the regulation of their levels in health and disease. *Curr Opin Lipidol* **18:**129–140.

Dinh TP, Carpenter D, Leslie FM, Freund TF, Katona I, Sensi SL, Kathuria S, and Piomelli D (2002) Brain monoglyceride lipase participating in endocannabinoid inactivation. *Proc Natl Acad Sci USA* **99:**10819–10824.

Ekholm ME, Johansson L, and Kukkonen JP (2007) IP_3-independent signalling of OX_1 orexin/hypocretin receptors to Ca^{2+} influx and ERK. *Biochem Biophys Res Commun* **353:**475–480.

Ellis J, Pediani JD, Canals M, Milasta S, and Milligan G (2006) Orexin-1 receptor-cannabinoid CB1 receptor heterodimerization results in both ligand-dependent and -independent coordinated alterations of receptor localization and function. *J Biol Chem* **281:**38812–38824.

Ghomashchi F, Naika GS, Bollinger JG, Aloulou A, Lehr M, Leslie CC, and Gelb MH (2010) Interfacial kinetic and binding properties of mammalian group IVB phospholipase A_2 (cPLA$_2\beta$) and comparison with the other cPLA2 isoforms. *J Biol Chem* **285:**36100–36111.

Ghosh M, Loper R, Ghomashchi F, Tucker DE, Bonventre JV, Gelb MH, and Leslie CC (2007) Function, activity, and membrane targeting of cytosolic phospholipase $A_2\zeta$ in mouse lung fibroblasts. *J Biol Chem* **282:**11676–11686.

Ghosh M, Tucker DE, Burchett SA, and Leslie CC (2006) Properties of the Group IV phospholipase A_2 family. *Prog Lipid Res* **45:**487–510.

Glass M, Hong J, Sato TA, and Mitchell MD (2005) Misidentification of prostamides as prostaglandins. *J Lipid Res* **46:**1364–1368.

Grimsey NL, Graham ES, Dragunow M, and Glass M (2010) Cannabinoid receptor 1 trafficking and the role of the intracellular pool: implications for therapeutics. *Biochem Pharmacol* **80:**1050–1062.

Håkansson M, de Lecea L, Sutcliffe JG, Yanagisawa M, and Meister B (1999) Leptin receptor- and STAT3-immunoreactivities in hypocretin/orexin neurones of the lateral hypothalamus. *J Neuroendocrinol* **11:**653–663.

Hilairet S, Bouaboula M, Carrière D, Le Fur G, and Casellas P (2003) Hypersensitization of the orexin 1 receptor by the CB1 receptor: evidence for cross-talk blocked by the specific CB1 antagonist, SR141716. *J Biol Chem* **278:**23731–23737.

Ho YC, Lee HJ, Tung LW, Liao YY, Fu SY, Teng SF, Liao HT, Mackie K, and Chiou LC (2011) Activation of orexin 1 receptors in the periaqueductal gray of male rats leads to antinociception via retrograde endocannabinoid (2-arachidonoylglycerol)-induced disinhibition. *J Neurosci* **31:**14600–14610.

Holmqvist T, Akerman KE, and Kukkonen JP (2002) Orexin signaling in recombinant neuron-like cells. *FEBS Lett* **526:**11–14.

Holmqvist T, Johansson L, Ostman M, Ammoun S, Akerman KE, and Kukkonen JP (2005) OX1 orexin receptors couple to adenylyl cyclase regulation via multiple mechanisms. *J Biol Chem* **280:**6570–6579.

Howlett AC (2005) Cannabinoid receptor signaling. *Handb Exp Pharmacol* **168:** 53–79.

Hu J and el-Fakahany EE (1993) Role of intercellular and intracellular communication by nitric oxide in coupling of muscarinic receptors to activation of guanylate cyclase in neuronal cells. *J Neurochem* **61:**578–585.

Huang H, Acuna-Goycolea C, Li Y, Cheng HM, Obrietan K, and van den Pol AN (2007) Cannabinoids excite hypothalamic melanin-concentrating hormone but inhibit hypocretin/orexin neurons: implications for cannabinoid actions on food intake and cognitive arousal. *J Neurosci* **27:**4870–4881.

Jäntti MH, Putula J, Somerharju P, Frohman MA, and Kukkonen JP (2012) OX_1 orexin/hypocretin receptor activation of phospholipase D. *Br J Pharmacol* **165:** 1109–1123.

Johansson L, Ekholm ME, and Kukkonen JP (2007) Regulation of OX_1 orexin/hypocretin receptor-coupling to phospholipase C by Ca^{2+} influx. *Br J Pharmacol* **150:**97–104.

Johansson L, Ekholm ME, and Kukkonen JP (2008) Multiple phospholipase activation by OX_1 orexin/hypocretin receptors. *Cell Mol Life Sci* **65:**1948–1956.

Kano M, Ohno-Shosaku T, Hashimotodani Y, Uchigashima M, and Watanabe M (2009) Endocannabinoid-mediated control of synaptic transmission. *Physiol Rev* **89:**309–380.

Kathuria S, Gaetani S, Fegley D, Valiño F, Duranti A, Tontini A, Mor M, Tarzia G, La Rana G, Calignano A, et al. (2003) Modulation of anxiety through blockade of anandamide hydrolysis. *Nat Med* **9:**76–81.

Kirkham TC, Williams CM, Fezza F, and Di Marzo V (2002) Endocannabinoid levels in rat limbic forebrain and hypothalamus in relation to fasting, feeding and satiation: stimulation of eating by 2-arachidonoyl glycerol. *Br J Pharmacol* **136:** 550–557.

Kukkonen JP (2011) A ménage à trois made in heaven: G-protein-coupled receptors, lipids and TRP channels. *Cell Calcium* **50:**9–26.

Kukkonen JP and Åkerman KEO (2005) Intracellular signal pathways utilized by the hypocretin/orexin receptors, in *Hypocretins as Integrators of Physiological Signals* (de Lecea L and Sutcliffe JG eds) pp 221–231, Springer Science+Business Media, Berlin.

Kukkonen JP, Holmqvist T, Ammoun S, and Akerman KE (2002) Functions of the orexinergic/hypocretinergic system. *Am J Physiol Cell Physiol* **283:**C1567–C1591.

Lee MW, Kraemer FB, and Severson DL (1995) Characterization of a partially purified diacylglycerol lipase from bovine aorta. *Biochim Biophys Acta* **1254:**311–318.

Long JZ, Li W, Booker L, Burston JJ, Kinsey SG, Schlosburg JE, Pavón FJ, Serrano AM, Selley DE, Parsons LH, et al. (2009) Selective blockade of 2-arachidonoylglycerol hydrolysis produces cannabinoid behavioral effects. *Nat Chem Biol* **5:**37–44.

López M, Seoane L, García MC, Lago F, Casanueva FF, Señarís R, and Diéguez C (2000) Leptin regulation of prepro-orexin and orexin receptor mRNA levels in the hypothalamus. *Biochem Biophys Res Commun* **269:**41–45.

Lund PE, Shariatmadari R, Uustare A, Detheux M, Parmentier M, Kukkonen JP, and Akerman KE (2000) The orexin OX_1 receptor activates a novel Ca^{2+} influx pathway necessary for coupling to phospholipase C. *J Biol Chem* **275:**30806–30812.

Minkkilä A, Savinainen JR, Käsnänen H, Xhaard H, Nevalainen T, Laitinen JT, Poso A, Leppänen J, and Saario SM (2009) Screening of various hormone-sensitive lipase inhibitors as endocannabinoid-hydrolyzing enzyme inhibitors. *ChemMedChem* **4:**1253–1259.

Mori K, Kim J, and Sasaki K (2011) Electrophysiological effects of orexin-B and dopamine on rat nucleus accumbens shell neurons in vitro. *Peptides* **32:**246–252.

Muccioli GG, Labar G, and Lambert DM (2008) CAY10499, a novel monoglyceride lipase inhibitor evidenced by an expeditious MGL assay. *Chembiochem* **9:**2704–2710.

Putula J and Kukkonen JP (2012) Mapping of the binding sites for the OX_1 orexin receptor antagonist, SB-334867, using orexin/hypocretin receptor chimaeras. *Neurosci Lett* **506:**111–115.

Savinainen JR, Saario SM, Niemi R, Järvinen T, and Laitinen JT (2003) An optimized approach to study endocannabinoid signaling: evidence against constitutive activity of rat brain adenosine A1 and cannabinoid CB1 receptors. *Br J Pharmacol* **140:**1451–1459.

Savinainen JR, Yoshino M, Minkkilä A, Nevalainen T, and Laitinen JT (2010) Characterization of binding properties of monoglyceride lipase inhibitors by a versatile fluorescence-based technique. *Anal Biochem* **399:**132–134.

Scammell TE and Winrow CJ (2011) Orexin receptors: pharmacology and therapeutic opportunities. *Annu Rev Pharmacol Toxicol* **51:**243–266.

Scott SA, Selvy PE, Buck JR, Cho HP, Criswell TL, Thomas AL, Armstrong MD, Arteaga CL, Lindsley CW, and Brown HA (2009) Design of isoform-selective phospholipase D inhibitors that modulate cancer cell invasiveness. *Nat Chem Biol* **5:**108–117.

Seno K, Okuno T, Nishi K, Murakami Y, Watanabe F, Matsuura T, Wada M, Fujii Y, Yamada M, Ogawa T, et al. (2000) Pyrrolidine inhibitors of human cytosolic phospholipase A_2. *J Med Chem* **43:**1041–1044.

Seno K, Okuno T, Nishi K, Murakami Y, Yamada K, Nakamoto S, and Ono T (2001) Pyrrolidine inhibitors of human cytosolic phospholipase A_2. 2. Synthesis of potent and crystallized 4-triphenylmethylthio derivative 'pyrrophenone.' *Bioorg Med Chem Lett* **11:**587–590.

Smart D, Jerman JC, Brough SJ, Rushton SL, Murdock PR, Jewitt F, Elshourbagy NA, Ellis CE, Middlemiss DN, and Brown F (1999) Characterization of recombinant human orexin receptor pharmacology in a Chinese hamster ovary cell-line using FLIPR. *Br J Pharmacol* **128:**1–3.

Song H, Ramanadham S, Bao S, Hsu FF, and Turk J (2006) A bromoenol lactone suicide substrate inactivates group VIA phospholipase A_2 by generating a diffus-

ible bromomethyl keto acid that alkylates cysteine thiols. *Biochemistry* **45:**1061–1073.
Soria-Gómez E, Matias I, Rueda-Orozco PE, Cisneros M, Petrosino S, Navarro L, Di Marzo V, and Prospéro-García O (2007) Pharmacological enhancement of the endocannabinoid system in the nucleus accumbens shell stimulates food intake and increases c-Fos expression in the hypothalamus. *Br J Pharmacol* **151:**1109–1116.
Taylor CW and Broad LM (1998) Pharmacological analysis of intracellular Ca^{2+} signalling: problems and pitfalls. *Trends Pharmacol Sci* **19:**370–375.
Tsuboi K, Hilligsmann C, Vandevoorde S, Lambert DM, and Ueda N (2004) *N*-Cyclohexanecarbonylpentadecylamine: a selective inhibitor of the acid amidase hydrolysing *N*-acylethanolamines, as a tool to distinguish acid amidase from fatty acid amide hydrolase. *Biochem J* **379:**99–106.
Turunen PM, Ekholm ME, Somerharju P, and Kukkonen JP (2010a) Arachidonic acid release mediated by OX_1 orexin receptors. *Br J Pharmacol* **159:**212–221.
Turunen PM, Putula J, and Kukkonen JP (2010b) Filtration assay for arachidonic acid release. *Anal Biochem* **407:**233–236.
Ward RJ, Pediani JD, and Milligan G (2011) Hetero-multimerization of the cannabinoid CB_1 receptor and the orexin OX_1 receptor generates a unique complex in which both protomers are regulated by orexin A. *J Biol Chem* **286:**37414–37428.
Zheng H, Corkern M, Stoyanova I, Patterson LM, Tian R, and Berthoud HR (2003) Peptides that regulate food intake: appetite-inducing accumbens manipulation activates hypothalamic orexin neurons and inhibits POMC neurons. *Am J Physiol Regul Integr Comp Physiol* **284:**R1436–R1444.

Address correspondence to: Dr. Jyrki P. Kukkonen, Biochemistry and Cell Biology, Department of Veterinary Biosciences, University of Helsinki, P.O. Box 66, FIN-00014, University of Helsinki, Helsinki, Finland. E-mail: jyrki.kukkonen@helsinki.fi